Supporting Information: How Do Methyl Groups Enhance the Triplet Chemiexcitation Yield of Dioxetane?

Morgane Vacher,[*,†] Pooria Farahani,[‡] Alessio Valentini,[¶] Luis Manuel Frutos,[§] Hans O. Karlsson,[†] Ignacio Fdez. Galván,[†] and Roland Lindh[*,†]

Department of Chemistry – Ångström, The Theoretical Chemistry Programme, Uppsala University, Box 538, 751 21 Uppsala, Sweden, Instituto de Química, Departamento de Química Fundamental, Universidade de São Paulo, C.P. 05508-000, São Paulo, Brazil, Département de Chimie, Université de Liège, Allée du 6 Août, 11, 4000 Liège, Belgium, and Departamento de Química Física, Universidad de Alcalá, E-28871 Alcalá de Henares, Madrid, Spain

E-mail: morgane.vacher@kemi.uu.se; roland.lindh@kemi.uu.se

[*]To whom correspondence should be addressed
[†]Uppsala University
[‡]Universidade de São Paulo
[¶]Université de Liège
[§]Universidad de Alcalá

Experimental triplet excitation yield upon decomposition of methyl-substituted dioxetane molecules

Figure S1 plots the experimental triplet excitation yields upon decomposition of methyl-substituted dioxetane molecules, measured by chemiluminescence measurements and chemical titrations.[1] See Figure 1 in the main text for the labelling of the compounds **a**-**e**. Compound **c'** corresponds to the isomer with two methyl groups bonded to different carbon atoms in position *cis*; compound **c''** corresponds to the isomer with two methyl groups on different carbon atoms in position *trans*.

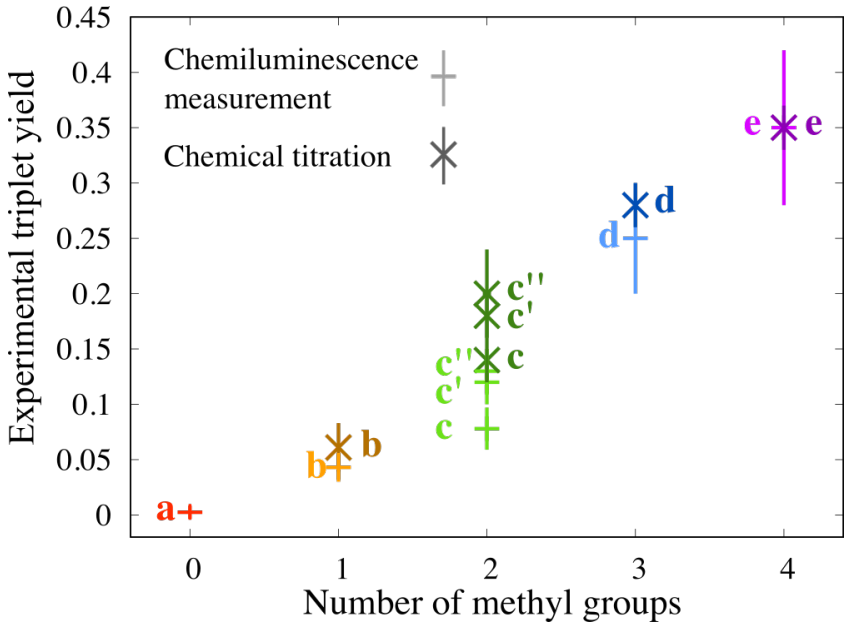

Figure S1: Measured triplet excitation yields upon decomposition of dioxetane molecules using chemiluminescent methods (bar) and chemical titration methods (cross). The data and error bars are taken from a previous experimental work.[1]

Transition state structures and initial nuclear velocities along the transition vectors for the studied compounds

The nuclear geometry of the transition state structures for the O–O bond breaking are given in Tables S1, S2, S3, S4 and S5 for the compounds **a**, **b**, **c**, **d** and **e** respectively (see Figure 1 of the main text for the labelling of the compounds). They were optimised at CASSCF(12,10)/ANO-RCC-VTZP level of theory[2–5] using a development version of the Molcas package.[6] Tables S6, S7, S8, S9 and S10 give the initial nuclear velocities along the transition vectors (equivalent to 1kcal/mol of kinetic energy towards the biradical product) for the compounds **a**, **b**, **c**, **d** and **e** respectively. The transition vectors were obtained by calculating the normal modes at the transition state structure, at the same level of theory as for the geometry optimisation.

Table S1: Compound a: Transition state structure for the O–O bond breaking optimised at CASSCF(12,10)/ANO-RCC-VTZP level of theory [Å].

Atom	x	y	z
C	-0.75188423	0.15702743	-0.62100275
H	-1.33038300	-0.44090287	-1.31225901
H	-0.93985370	1.21031672	-0.77447566
C	0.75188426	-0.15702747	-0.62100257
H	0.93985382	-1.21031676	-0.77447539
H	1.33038305	0.44090285	-1.31225878
O	-1.10698084	-0.22955661	0.71807154
O	1.10698064	0.22955673	0.71807174

Table S2: Compound b: Transition state structure for the O–O bond breaking optimised at CASSCF(12,10)/ANO-RCC-VTZP level of theory [Å].

Atom	x	y	z
C	-0.76232738	0.15554998	-0.53577466
H	-1.36812994	-0.73971404	-0.48576564
H	-1.14160748	0.83210088	-1.29057541
C	0.73093025	-0.18328385	-0.70117323
H	1.27224411	0.70365977	-1.00524875
C	1.05540854	-1.36008412	-1.59447315
O	-0.76673783	0.84141998	0.72335484
O	1.08729780	-0.50748691	0.65869033
H	0.78672547	-1.13218413	-2.61913404
H	2.11589141	-1.57560867	-1.56680990
H	0.51596134	-2.24447501	-1.28110881

Table S3: Compound c: Transition state structure for the O–O bond breaking optimised at CASSCF(12,10)/ANO-RCC-VTZP level of theory [Å].

Atom	x	y	z
C	-0.81527530	0.20619161	-0.51234732
C	0.68148620	-0.09243049	-0.78722337
H	1.23353108	0.81862789	-0.97334281
O	-0.73634818	0.60005849	0.88148262
O	1.11866991	-0.70373027	0.43080768
C	-1.35075211	1.39530858	-1.29055361
H	-1.37186648	1.16926612	-2.34998732
H	-2.36133011	1.62759909	-0.97842644
H	-0.73405188	2.27005044	-1.13417116
H	0.84133777	-0.80233560	-1.58877823
C	-1.68384524	-1.03272427	-0.65586115
H	-2.68241002	-0.83131174	-0.28946040
H	-1.75502685	-1.33314066	-1.69530230
H	-1.27181456	-1.85332928	-0.08507339

Table S4: Compound d: Transition state structure for the O–O bond breaking optimised at CASSCF(12,10)/ANO-RCC-VTZP level of theory [Å].

Atom	x	y	z
C	-0.82343611	0.15757959	-0.47903345
C	0.68659192	-0.20394982	-0.63568735
H	1.23541120	0.72082990	-0.76252324
C	1.07496817	-1.19852225	-1.71120915
O	-0.80458640	0.70080116	0.86158583
O	1.02934865	-0.76736018	0.63865889
H	0.80999182	-0.81273513	-2.68791602
H	2.14532254	-1.35866934	-1.69518261
H	0.58546479	-2.15173226	-1.56934366
C	-1.26538202	1.27747557	-1.40742836
H	-1.25939726	0.93751723	-2.43594598
H	-2.27357185	1.59127895	-1.16722318
H	-0.61169999	2.13499401	-1.32043884
C	-1.75564030	-1.04279479	-0.52950767
H	-2.74667508	-0.74186525	-0.21472023
H	-1.82750351	-1.44575851	-1.53250577
H	-1.41327154	-1.82257530	0.13647894

Table S5: Compound e: Transition state structure for the O–O bond breaking optimised at CASSCF(12,10)/ANO-RCC-VTZP level of theory [Å].

Atom	x	y	z
C	-0.80540828	0.21009608	-0.54913558
C	0.71614626	-0.13405381	-0.80407237
C	0.96958595	-1.24884391	-1.81024377
O	-0.73699757	0.83383456	0.75156558
O	1.10585811	-0.65216967	0.48647537
H	0.60901628	-0.95751618	-2.78923376
H	2.03271784	-1.43632266	-1.89026310
H	0.48521235	-2.16970551	-1.52272039
C	-1.40317419	1.24541241	-1.49265930
H	-1.39548865	0.87241437	-2.50957959
H	-2.43192853	1.44122109	-1.21859621
H	-0.86223757	2.17907627	-1.46218500
C	-1.69162364	-1.02562837	-0.45779368
H	-2.65892846	-0.73576986	-0.06877737
H	-1.84084332	-1.47992950	-1.42944243
H	-1.26679205	-1.76056034	0.21052109
C	1.56255322	1.09270892	-1.11932164
H	2.60858158	0.82119077	-1.06353725
H	1.36358027	1.46691655	-2.11588217
H	1.38184866	1.88377960	-0.40601898

Table S6: Compound a: Initial velocities along the transition vector [a.u. of velocity], equivalent to a kinetic energy of 1 kcal/mol. The transition vector was obtained at the transition state structure for the O–O bond breaking, at CASSCF(12,10)/ANO-RCC-VTZP level of theory.

Atom	x	y	z
C	-6.16546E-06	9.66976E-06	5.8124E-05
H	5.92833E-05	5.02195E-05	-3.55305E-05
H	2.12629E-05	1.82329E-05	7.44071E-05
C	6.11277E-06	-9.61707E-06	5.82557E-05
H	-2.15923E-05	-1.82593E-05	7.44466E-05
H	-5.9033E-05	-5.04303E-05	-3.5346E-05
O	-0.000213934	-5.34208E-05	-4.60961E-05
O	0.000213973	5.33945E-05	-4.61356E-05

Table S7: Compound b: Initial velocities along the transition vector [a.u. of velocity], equivalent to a kinetic energy of 1 kcal/mol. The transition vector was obtained at the transition state structure for the O–O bond breaking, at CASSCF(12,10)/ANO-RCC-VTZP level of theory.

Atom	x	y	z
C	7.14043E-06	-1.46629E-05	5.48574E-05
H	2.58215E-05	-2.72443E-05	8.18646E-05
H	4.57277E-05	-9.92809E-05	-4.36725E-05
C	2.75078E-05	-9.93336E-06	6.71753E-05
H	1.2858E-05	1.87074E-06	7.08773E-05
C	-2.0723E-05	2.48598E-05	-1.18041E-05
O	-0.000177457	0.00013273	-5.4449E-05
O	0.000167866	-0.000131558	-3.01426E-05
H	-6.46722E-05	7.00473E-05	1.08951E-05
H	-2.13949E-05	1.87864E-05	-6.33943E-05
H	-1.1949E-05	1.40832E-05	-2.64538E-05

Table S8: Compound c: Initial velocities along the transition vector [a.u. of velocity], equivalent to a kinetic energy of 1 kcal/mol. The transition vector was obtained at the transition state structure for the O–O bond breaking, at CASSCF(12,10)/ANO-RCC-VTZP level of theory.

Atom	x	y	z
C	-1.11585E-05	1.38460E-05	5.86E-05
C	9.77518E-06	2.03540E-05	5.74E-05
H	-6.45531E-07	3.67557E-05	1.00E-04
O	-1.80814E-04	1.14457E-04	6.64E-06
O	1.56139E-04	-1.34890E-04	-0.000103021
C	1.80090E-05	-1.20016E-05	-1.60E-05
H	6.05086E-05	-5.12209E-05	-7.54E-06
H	6.38944E-06	-4.80854E-06	-6.12E-05
H	8.97156E-06	-3.92588E-06	-2.36E-05
H	-3.61102E-05	1.01941E-04	-2.70E-05
C	9.09012E-06	-3.42526E-07	2.55E-05
H	-9.65661E-06	-8.91886E-06	-2.27E-05
H	6.52118E-05	-1.31741E-05	2.54E-05
H	-9.27456E-06	7.23258E-06	5.16E-05

Table S9: Compound d: Initial velocities along the transition vector [a.u. of velocity], equivalent to a kinetic energy of 1 kcal/mol. The transition vector was obtained at the transition state structure for the O–O bond breaking, at CASSCF(12,10)/ANO-RCC-VTZP level of theory.

Atom	x	y	z
C	-6.82419E-06	8.87935E-06	5.05491E-05
C	1.24891E-05	-1.09872E-05	6.83736E-05
H	1.92210E-05	-8.27334E-06	1.09042E-04
C	-2.30679E-05	5.02329E-05	-1.61515E-05
O	-1.68773E-04	1.27683E-04	-2.45434E-05
O	1.51924E-04	-1.45982E-04	-5.65696E-05
H	-8.96235E-05	8.28256E-05	1.67179E-05
H	-1.95372E-05	7.53559E-05	-7.75691E-05
H	8.32604E-06	3.15520E-05	-3.06298E-05
C	3.33700E-05	-2.81135E-05	-2.66380E-05
H	7.07581E-05	-7.04288E-05	-1.10136E-05
H	2.58871E-05	-1.75084E-05	-7.39331E-05
H	3.01160E-05	-2.40954E-05	-3.70192E-05
C	1.52820E-06	-4.08397E-07	3.33437E-05
H	-1.43993E-05	-1.00123E-06	-1.79827E-05
H	5.22749E-05	-2.56236E-05	4.04313E-05
H	-2.37529E-05	1.42149E-05	6.57915E-05

Table S10: Compound e: Initial velocities along the transition vector [a.u. of velocity], equivalent to a kinetic energy of 1 kcal/mol. The transition vector was obtained at the transition state structure for the O–O bond breaking, at CASSCF(12,10)/ANO-RCC-VTZP level of theory.

Atom	x	y	z
C	-7.77263E-07	1.37009E-05	4.65567E-05
C	1.63884E-05	-9.84094E-06	4.40668E-05
C	-2.65850E-05	2.73886E-05	-2.12232E-05
O	-1.70550E-04	1.30396E-04	-3.04582E-05
O	1.52238E-04	-1.34875E-04	-7.67382E-05
H	-9.15194E-05	5.33676E-05	1.18302E-05
H	-2.85743E-05	4.89017E-05	-8.42342E-05
H	5.74384E-06	8.76067E-06	-2.38053E-05
C	1.80747E-05	-2.95492E-05	-2.68880E-05
H	9.15326E-05	-5.42108E-05	-1.60327E-05
H	-1.84435E-06	-5.62527E-05	-8.71456E-05
H	-1.43596E-05	-1.00781E-05	-2.11442E-05
C	7.02171E-06	4.88753E-06	4.77028E-05
H	-8.22054E-06	3.42523E-07	1.04865E-05
H	4.90202E-05	-1.80220E-05	5.27485E-05
H	-4.78214E-06	1.90100E-05	7.30363E-05
C	9.45889E-06	-7.24567E-07	4.78082E-05
H	1.07631E-05	-2.50305E-07	7.71993E-06
H	-2.79156E-05	2.33311E-05	6.51978E-05
H	2.99707E-05	-1.33716E-05	6.92818E-05

Derivation and assumptions of the kinetic model

Transfer of population between the manifold of four singlet states S and four triplet states T occurs in the entropic trap region, where the electronic states are close-to-degenerate. It is noted that what follows is independent on the actual number of singlet and triplet states (as long as they are the same). Considering explicitly the three components of the triplet states, we have: $S \longleftrightarrow T_1$, $S \longleftrightarrow T_2$ and $S \longleftrightarrow T_3$. Initially, $[S] = 1$ and $[T_1] = [T_2] = [T_3] = 0$ (Table S11). We assume the same rate constant k for all forward and backward transfers of population. As a consequence, the three components of the triplet states are equally populated $[T_1] = [T_2] = [T_3] = [T_i]$. Assuming first order reactions, we obtain:

$$\forall i, \frac{d[T_i]}{dt} = k([S] - [T_i])$$

$$\frac{d[S]}{dt} = 3k([T_i] - [S])$$

After integration, it reads:

$$\forall i, [T_i] = \frac{1}{4}\left(1 - \exp(-4kt)\right)$$

Therefore, the total population in the triplet states is:

$$x = [T] = 3[T_i] = \frac{3}{4}\left(1 - \exp(-4kt)\right)$$

If the system stayed an infinitely long time in the entropic trap, it would distribute equally among the degenerate S and three components of T (Table S11). It is noted that subsequent dissociation of the dioxetane molecule after the entropic trap region and emission of fluorescence / phosphorescence are beyond the present simple kinetic model.

Table S11: Transfer of population between S and T.

Time spent in the entropic trap	S $\longleftrightarrow$	T $(T_1 + T_2 + T_3)$
$t = 0$	1	0
$t > 0$	$1 - x$	x
$t = \infty$	0.25	0.75

References

(1) Adam, W.; Baader, W. J. Effects of methylation on the thermal stability and chemiluminescence properties of 1,2-dioxetanes. *J. Am. Chem. Soc.* **1985**, *107*, 410–416.

(2) Roos, B. O.; Taylor, P. R.; Siegbahn, P. E. A complete active space SCF method (CASSCF) using a density matrix formulated super-CI approach. *Chem. Phys.* **1980**, *48*, 157–173.

(3) Roos, B. O. The complete active space self-consistent field method and its applications in electronic structure calculations. *Adv. Chem. Phys.* **1987**, *69*, 399–446.

(4) Roos, B. O.; Lindh, R.; Malmqvist, P.-Å.; Veryazov, V.; Widmark, P.-O. Main Group Atoms and Dimers Studied with a New Relativistic ANO Basis Set. *J. Phys. Chem. A* **2004**, *108*, 2851–2858.

(5) Aquilante, F.; Gagliardi, L.; Pedersen, T. B.; Lindh, R. Atomic Cholesky decompositions: A route to unbiased auxiliary basis sets for density fitting approximation with tunable accuracy and efficiency. *J. Chem. Phys.* **2009**, *130*, 154107.

(6) Aquilante, F.; Autschbach, J.; Carlson, R. K.; Chibotaru, L. F.; Delcey, M. G.; De Vico, L.; Fdez. Galván, I.; Ferré, N.; Frutos, L. M.; Gagliardi, L. et al. Molcas 8: New capabilities for multiconfigurational quantum chemical calculations across the periodic table. *J. Comput. Chem.* **2016**, *37*, 506–541.